Available online at www.sciencedirect.com
ScienceDirect
Proceedings of the Combustion Institute 31 (2007) 2903–2911
Proceedings of the Combustion Institute
www.elsevier.com/locate/proci

Flamelet-based modeling of auto-ignition with thermal inhomogeneities for application to HCCI engines

David J. Cook [a,*], Heinz Pitsch [a], Jacqueline H. Chen [b], Evatt R. Hawkes [b]

[a] *Department of Mechanical Engineering, Stanford University, Stanford, CA 94305, USA*
[b] *Combustion Research Facility, Sandia National Laboratories, Livermore, CA 94551, USA*

Abstract

Homogeneous-charge compression ignition (HCCI) engines have been shown to have higher thermal efficiencies and lower NO_x and soot emissions than spark ignition engines. However, HCCI engines experience very large heat release rates which can cause too rapid an increase in pressure. One method of reducing the maximum heat release rate is to introduce thermal inhomogeneities, thereby spreading the heat release over several crank angle degrees. Direct numerical simulations (DNS) with complex H_2/air chemistry by Cook and Pitsch [D.J. Cook, H. Pitsch, *Western States Section of the Combustion Institute*, Boise, Idaho 06S-08, 2006] showed that both ignition fronts and deflagration-like fronts may be present in systems with such inhomogeneities. Here, an enthalpy-based flamelet model is presented and applied to the four cases of varying initial temperature variance presented in Cook and Pitsch [D.J. Cook, H. Pitsch, *Western States Section of the Combustion Institute*, Boise, Idaho 06S-08, 2006]. This model uses a mean scalar dissipation rate to model mixing between regions of higher and lower enthalpies. The predicted heat release rates agree well with the heat release rates of the four DNS cases. The model is shown to be capable of capturing the combustion characteristics for the case in which combustion occurs primarily in the form of spontaneous ignition fronts, for the case dominated by deflagration-type burning, and for the mixed mode cases. The enthalpy-based flamelet model shows considerably improved agreement with the DNS results over the popular multi-zone model, particularly, where both deflagrative and spontaneous ignition are occurring, that is, where diffusive transport is important.

Keywords: Ignition; HCCI; Flamelet model

1. Introduction

Homogeneous-charge compression ignition (HCCI) engines have recently been the subject of much research effort for both their low NO_x (oxides of nitrogen) and soot emissions, and higher thermal efficiency compared to spark ignition (SI) engines. While significant progress has been made, these engines continue to suffer from high carbon monoxide (CO) and unburnt hydrocarbon (UHC) emissions [1]. Additionally, HCCI engines experience high heat release rates, which

* Corresponding author. Fax: +1 925 294 2595.
E-mail addresses: david.cook@stanford.edu (D.J. Cook), erhawke@ca.sandia.gov (E.R. Hawkes).

1540-7489/$ - see front matter © 2006 Published by Elsevier Inc. on behalf of The Combustion Institute.
doi:10.1016/j.proci.2006.07.252

sometimes can lead to too rapid a pressure rise. Both the CO and UHC emissions and the heat release rates are strongly related to the level of temperature and mixture composition inhomogeneities in the cylinder gases.

While HCCI refers to a type of combustion which typically has an approximately homogeneous charge in terms of mixture composition, the charge experiences large stratification in the enthalpy field due to wall heat loss or heating because of hot valves combined with incomplete turbulent mixing between the bulk gases and gases in near wall regions. This stratification typically causes regions in the center of the cylinder to ignite first, followed later by regions closer to the cylinder walls. This stratification can lead to the occurrence of both volumetric and front-like combustion modes [2]. HCCI engines also have stratification of mixture composition due to incomplete mixing of the Exhaust Gas Recirculation (EGR) and the fresh charge, or due to late phased Direct Injection (DI). Here, only the effects of thermal inhomogeneities will be considered. These effects on CO and UHC emissions and on heat release rates will be briefly discussed below.

The relatively high CO emissions in HCCI engines are a consequence of the strategy used to achieve the main goal of reducing NO_x. Experimentally, it has been found that CO emissions originate in regions where the gas temperature does not exceed 1500 K [3]. Yet, in order to limit NO_x emissions, HCCI engines are run in a way that achieves low peak temperatures. This is generally accomplished by running the engines very lean or, more commonly, highly diluted with significant internal or external EGR. Such operating strategies can result in a maximum burnt gas temperature below 1850 K, and therefore lead to low NO_x emissions. Having a maximum burnt gas temperature below 1850 K in the cylinder implies that regions strongly affected by wall heat loss conditions will be favorable for producing higher CO emissions.

Unburnt hydrocarbon emissions come from regions in the cylinder where auto-ignition does not occur. These regions are typically either extremely dilute, as in the case of a partially stratified charge from direct injection, or are strongly affected by wall heat loss, or both. Another major cause of UHC emissions is cycles in which misfire occurs. Although, this cause of UHC emissions will likely become less significant with future improvements in operation control, it will still be important to model misfire correctly in the design of new engines and the development of novel control strategies.

The presence of thermal inhomogeneities tends to decrease the maximum heat release rates by spreading it over several crank angle degrees. One possible strategy to suppress overly rapid pressure rise is to introduce inhomogeneities of temperature or mixture fraction in order to produce the desired heat release rate [4]. A charge with non-negligible levels of thermal inhomogeneities will have some hot and some cold regions. Gas in the hot regions will tend to ignite first, followed by regions that are a little cooler, until finally, the gas in the cold regions ignites. Turbulence in the engine will also mix these regions on large and smaller scales, so that the thermal stratifications occur on all turbulent scales. The larger the level of inhomogeneity, the lower the maximum heat release rates will be.

Thus, thermal inhomogeneities affect the combustion emissions and heat release rates in HCCI engines. As experimental data suggest that cylinder flow and turbulence play an important role in HCCI combustion [5], a better understanding of its interaction with chemical kinetics could be used to reduce CO and UHC emissions and control the heat release rates in HCCI engines. These effects have been modeled using multiple zones, where ignition of gas with a smaller enthalpy defect (i.e., gases less affected by wall heat loss) affects gases with higher levels of enthalpy defect only through the increased pressure associated with the volumetric expansion of the ignited gases [6–8]. Additionally, fully coupled CFD and chemistry studies have been done, in which the chemical source terms have been evaluated using mean values, and a low-order correction for the effects of turbulence have been used in the combustion process [9]. In the present study, the effect of thermal inhomogeneities on combustion is modeled using a flamelet-like approach proposed by Cook et al. [10] and Cook and Pitsch [11]. In this model, the flamelet-type equations are solved in a normalized enthalpy space. Transport across this enthalpy space physically represents interaction between gases of higher and lower levels of enthalpy defect. The model is validated using DNS data of constant volume auto-ignition of H_2/air with thermal inhomogeneities conducted by Refs. [12,13]. Results are also compared with an idealized multi-zone model [14].

2. Enthalpy-based flamelet modeling

In this section, a derivation of the enthalpy-based flamelet equations will be given. The low Mach number transport equations for species mass-fractions and total enthalpy are as follows

$$\rho\frac{\partial Y_i}{\partial t}+\rho v_j\frac{\partial Y_i}{\partial x_j}=\frac{\partial}{\partial x_j}\left[\rho D\frac{\partial Y_i}{\partial x_j}\right]+\rho\dot{\omega}_i, \tag{1}$$

$$\rho\frac{\partial H}{\partial t}+\rho v_j\frac{\partial H}{\partial x_j}=\frac{\partial}{\partial x_j}\left[\rho D\frac{\partial H}{\partial x_j}\right]+\frac{\partial p}{\partial t}-\dot{q}_{\Delta h}, \tag{2}$$

where Y_i is the mass fraction of species i, H is the total enthalpy, ρ is the density, D is the molecular

diffusivity assumed equal for all species, $\dot{\omega}_i$ is the chemical source term for species i, p is the pressure, $\dot{q}_{\Delta h}$ accounts for volumetric heat loss such as radiation, and v_j is the velocity in the x_j-direction. The term total enthalpy here refers to an enthalpy defined as

$$H = \sum_i Y_i h_i, \tag{3}$$

where h_i are the species enthalpies defined to include the heats of formation.

Since the enthalpy here is the main parameter leading to local changes in the auto-ignition behavior, the (x_1, x_2, x_3)-coordinate system will be transformed into a system which locally aligns with the enthalpy gradients. In the following analysis of this transformation, the x_1-coordinate is assumed to be normal, and the x_2- and x_3-coordinates are assumed to be tangential to an iso-enthalpy surface. This transformation is made such that

$$(t, x_1, x_2, x_3) \rightarrow (\tau, H, H_2, H_3), \tag{4}$$

where enthalpy is introduced as a new independent coordinate. This implies that the new independent coordinate, H, is attached to an iso-surface of enthalpy and that the new coordinates H_2 and H_3 lie within this surface. Hence, the transformation leads to

$$\frac{\partial}{\partial t} = \frac{\partial}{\partial \tau} + \frac{\partial H}{\partial t}\frac{\partial}{\partial H}, \tag{5}$$

$$\nabla = \nabla H \frac{\partial}{\partial H} + \nabla_{H\perp}, \quad \text{with } \nabla_{H\perp} = \begin{pmatrix} 0 \\ \partial/\partial H_2 \\ \partial/\partial H_3 \end{pmatrix}. \tag{6}$$

Applying Eqs. (5) and (6) to Eq. (1) and making use of Eq. (2) to cancel terms results in the transformed form of the equations,

$$\begin{aligned} \rho \frac{\partial Y_i}{\partial \tau} = &- \left[\frac{\partial p}{\partial t} - \dot{q}_{\Delta h}\right]\frac{\partial Y_i}{\partial H} - \rho v_j \nabla_{H\perp} Y_i \\ &+ \frac{\rho \chi_H}{2}\frac{\partial^2 Y_i}{\partial H^2} + \nabla_{H\perp}[\rho D \nabla_{H\perp} Y_i] \\ &+ \nabla H \frac{\partial}{\partial H}[\rho D \nabla_{H\perp} Y_i] \\ &+ \rho D \nabla H \nabla_{H\perp}\left[\frac{\partial Y_i}{\partial H}\right] + \rho \dot{\omega}_i, \end{aligned} \tag{7}$$

where the scalar dissipation rate in enthalpy-space was introduced as,

$$\chi_H \equiv 2D \frac{\partial H}{\partial x_j}\frac{\partial H}{\partial x_j}. \tag{8}$$

The first term on the right hand side of Eq. (7) represents a convection term in enthalpy space. This term is not present in the mixture fraction formulation of the flamelet equations because mixture fraction is a conserved scalar, while enthalpy is not. The temperature equation can similarly be expressed in enthalpy space and is here omitted for brevity.

2.1. Asymptotic analysis

Two different regimes of auto-ignition in HCCI engines can be identified [1]. For the first, chemical kinetics are the dominate physical process with mixing and heat transfer only influencing initial conditions for combustion. Experimental support for this viewpoint exists for 4-stroke HCCI engines with low levels of stratification [15–17]. In the second, mixing influences combustion on a microscopic level and under some circumstances, found mostly in DI engines with high levels of stratification, combustion is limited by mixing [18,19]. Recently, there has been a move toward operating HCCI engines under more stratified conditions in order to achieve desired engine operating characteristics such as lower emissions through direct injection, higher power from 2-stroke engines [20], and suppress the occurrence of too rapid pressure rise and lower peak pressures through extended heat release rates [4].

Hence, we will consider these regimes first independently, and finally for both regimes.

2.1.1. Homogeneous reactor regime

For all HCCI engines, some level of either thermal or charge stratification exists. Heat losses at the cylinder walls create thermal boundary layers which along with the hotter gasses in the center of the cylinder represent thermal stratification. For sufficiently low levels of stratification or sufficiently long stratification length-scales, molecular mixing effects are small [21,22]. In this limit, combustion is dominated by chemical kinetics and different locations in the cylinder can be reasonably approximated as homogeneous reactors which only interact by pressure work. While it is uncertain that an HCCI engine ever operates in this limit, this modeling strategy has been successfully advanced and widely used in the form of multi-zone models [6–8]. In this section, an asymptotic analysis of this limit will be applied to Eq. (7).

For the case of chemical kinetics dominated flow, spatial changes are small. Introducing a normalized coordinate $\overline{\boldsymbol{x}} = \epsilon \boldsymbol{x}$, the coordinate transformation, Eq. (4), becomes $t, \overline{x}_1, \overline{x}_2, \overline{x}_3 \rightarrow \tau, H, \overline{H}_2, \overline{H}_3$ with $\overline{H}_{2,3} = \epsilon H_{2,3}$. Then, for Eq. (6) follows

$$\nabla = \epsilon \overline{\nabla}\frac{\partial}{\partial H} + \epsilon \nabla_{\overline{H}\perp}, \tag{9}$$

and the transformation yields

$$\rho\frac{\partial Y_i}{\partial\tau} = -\left[\frac{\partial p^*}{\partial t} - \dot{q}_{\Delta h}\right]\frac{\partial Y_i}{\partial H} + \rho\dot{\omega}_i^* + \epsilon^2\rho D\overline{\nabla}^2\frac{\partial^2 Y_i}{\partial H^2} + \epsilon^2\nabla_{\overline{H}\perp}\left[\rho D\nabla_{\overline{H}\perp}Y_i\right] + \epsilon^2\rho D\overline{\nabla}\nabla_{\overline{H}\perp}\left[\frac{\partial Y_i}{\partial H}\right] - \epsilon\rho v_j\nabla_{\overline{H}\perp}Y_i + \epsilon^2\overline{\nabla}\frac{\partial}{\partial H}\left[\rho D\nabla_{\overline{H}\perp}Y_i\right]. \quad (10)$$

Since in the limit of auto-ignition without spatial enthalpy variations, implying $\epsilon \to 0$, both the accumulation term and the chemical source term have to remain, the scaling for these terms has been chosen appropriately. Then, keeping only the leading order terms leads to

$$\rho\frac{\partial Y_i}{\partial\tau} + \left[\frac{\partial p}{\partial t} - \dot{q}_{\Delta h}\right]\frac{\partial Y_i}{\partial H} = \rho\dot{\omega}_i. \quad (11)$$

Solution of Eq. (11) over the range of enthalpies representative of an HCCI engine would represent a multi-zone type modeling approach. Note that Eq. (11) is different from simply neglecting the diffusion term in Eq. (1), because of the different coordinate system that is attached to iso-enthalpy surfaces. It is also interesting to note that the convection term along iso-enthalpy surfaces appearing in Eq. (10) is $\mathcal{O}(\epsilon)$, and hence more important than the diffusive transport terms, which are $\mathcal{O}(\epsilon^2)$. If the velocity fluctuations occur on a scale larger than an ignition kernel, this convection term could be considered in a Lagrangian description. Otherwise, this term is responsible for turbulent mixing within the ignition kernel.

2.1.2. Propagating diffusive front regime

For the limit of large spatial enthalpy gradients, spatial variations in the direction of the enthalpy gradient are large compared to changes along iso-enthalpy surfaces. Then, an analysis very similar to the flamelet analysis of Refs. [23,24] can be carried out. A stretched enthalpy-coordinate can be introduced such that

$$\zeta = \varepsilon^{-1}(H - H_{\text{ref}}) \quad (12)$$

$$\zeta_{2,3} = H_{2,3}. \quad (13)$$

Then, from Eq. (6) follows

$$\nabla = \varepsilon^{-1}\nabla H\frac{\partial}{\partial\zeta} + \nabla_{\zeta\perp}, \quad (14)$$

Introducing this into Eq. (7) yields

$$\varepsilon^{-2}\rho\frac{\partial Y_i}{\partial\tau^*} = -\varepsilon^{-2}\frac{\partial Y_i}{\partial\zeta}\left[\frac{\partial p^*}{\partial t} - \dot{q}^*_{\Delta h}\right] + \varepsilon^{-2}\frac{\rho\chi_H}{2}\frac{\partial^2 Y_i}{\partial\zeta^2} + \varepsilon^{-2}\rho\ \dot{\omega}^*{}_i + \varepsilon^{-1}\nabla H\frac{\partial}{\partial\zeta}[\rho D\nabla_{\zeta\perp}Y_i] - \varepsilon^{-1}\rho v_j\nabla_{\zeta\perp}Y_i + \nabla_{\zeta\perp}[\rho D\nabla_{\zeta\perp}Y_i] + \varepsilon^{-1}\rho D\nabla H\nabla_{\zeta\perp}\left[\frac{\partial Y_i}{\partial\zeta}\right]. \quad (15)$$

The scalings for the accumulation term, the chemical source term, and the pressure term have been chosen such that these terms are of leading order. The former two have to remain for an auto-ignition problem, the latter to ensure energy conservation.

Retaining only the leading order terms in Eq. (15), results in flamelet-type equations in enthalpy space given by,

$$\rho\frac{\partial Y_i}{\partial\tau} + \left[\frac{\partial p}{\partial t} - \dot{q}_{\Delta h}\right]\frac{\partial Y_i}{\partial H} = \frac{\rho\chi_H}{2}\frac{\partial^2 Y_i}{\partial H^2} + \rho\dot{\omega}_i. \quad (16)$$

The difference between Eqs. (16) and (11) is that the former includes diffusive transport in the enthalpy direction. However, Eq. (16) reduces to Eq. (11) in the limit of low levels of thermal stratification.

2.2. Nondimensionalization

In order to simplify the numeric solution of the these equations, the enthalpy coordinate will be normalized by defining a new coordinate ξ as

$$\xi = \frac{H - \Theta_0(\tau)}{\Theta_1(\tau) - \Theta_0(\tau)} = \frac{H - \Theta_0(\tau)}{\Delta\Theta(\tau)}. \quad (17)$$

$\Theta_0(\tau)$ and $\Theta_1(\tau)$ represent the minimum and maximum enthalpies in the system so that $0 \leqslant \xi \leqslant 1$.

Now a simple coordinate transformation is performed to transform the enthalpy-based flamelet equations from H and τ space into ξ and τ^* space. The transformation rules are as follows,

$$\frac{\partial}{\partial\tau} = \frac{\partial}{\partial\tau^*} + \frac{\partial\xi}{\partial\tau}\frac{\partial}{\partial\xi} \quad (18)$$

$$\frac{\partial}{\partial H} = \frac{\partial\xi}{\partial H}\frac{\partial}{\partial\xi}. \quad (19)$$

In order to simplify this transformation a new variable, which represents a convective velocity in ξ-space, is introduced as

$$v_\xi = \frac{1}{\rho\Delta\Theta}\left[\frac{\partial p}{\partial t} - \dot{q}_{\Delta h}\right] - \frac{(1-\xi)}{\Delta\Theta}\frac{\partial\Theta_0}{\partial\tau} - \frac{\xi}{\Delta\Theta}\frac{\partial\Theta_1}{\partial\tau}. \quad (20)$$

Applying the transformation rules in Eqs. (18) and (19) to the enthalpy space flamelet equations given by Eq. (7) results in the normalized enthalpy-based flamelet equations in final form as given by

$$\rho\frac{\partial Y_i}{\partial \tau^*} = -\rho v_\xi \frac{\partial Y_i}{\partial \xi} + \frac{\rho\chi_\xi}{2}\frac{\partial^2 Y_i}{\partial \xi^2} + \rho\dot{\omega}_i \tag{21}$$

$$\begin{aligned}\rho\frac{\partial T}{\partial \tau^*} = &-\rho v_\xi \frac{\partial T}{\partial \xi} + \frac{\rho\chi_\xi}{2}\frac{\partial^2 T}{\partial \xi^2} + \frac{1}{C_p}\left[\frac{\partial p}{\partial t} - \dot{q}_{\Delta h}\right] \\ &+ \frac{\rho\chi_\xi}{2C_p}\frac{\partial T}{\partial \xi}\left(\frac{\partial C_p}{\partial \xi} + \sum_i^{\mathrm{N}} c_{p,i}\frac{\partial Y_i}{\partial \xi}\right) \\ &- \frac{\rho}{C_p}\sum_i^{\mathrm{N}} h_i\dot{\omega}_i.\end{aligned} \tag{22}$$

Here, C_p represents the specific heat of the mixture. Note that in the application of the model, the temperature equation in Eq. (21) can be replaced by the definition of the enthalpy, Eq. (3).

3. Numerical simulations

3.1. Direct numerical simulation

To validate this modeling approach, DNS results of the auto-ignition of a lean hydrogen-air mixture in a closed volume in the presence of an inhomogeneous initial temperature field by Refs. [12,13] are used. The initial conditions include a uniform mixture composition field with equivalence ratio of 0.1, initial pressure of 41 atm, mean initial temperature of 1070 K, and a turbulent Reynolds number of 213.5. Further details of the DNS code, the initialization, and computational grid can be found in Ref. [12]. The DNS used a detailed H_2/air chemical mechanism by Mueller et al. [25] with nine species and 42 reactions. Five different cases are studied here. The first four cases are identical, except that each had a different level of thermal stratification. The root-mean-square values of the initial temperature fluctuations, T', were 3.75, 7.5, 15, and 30 K for the four cases, respectively. All these cases have been computed considering differential diffusion by using non-unity Lewis numbers. A fifth case was computed at the conditions of case 3 (T' of 15 K), but using unity Lewis numbers for all species. A summary of all five cases is given in Table 1.

Table 1
Summary of conditions for all DNS cases

Case	T' (K)	Differential diffusion
1	3.75	Yes
2	7.5	Yes
3	15	Yes
4	30	Yes
5	15	No

3.2. Modeled simulations

A fully implicit one-dimensional finite difference code was used to solve the combustion model, Eqs. (21) and (22). An equidistant grid of 101 points in ξ-space was used. The maximum and minimum enthalpies, Θ_1 and Θ_0, were taken from the DNS. Additionally, the enthalpy dissipation rate, χ_H, as defined by Eq. (8), appears as a parameter in the enthalpy-based flamelet equations. For this study, it was taken from the DNS data as the mean enthalpy dissipation rate conditioned on enthalpy. Furthermore, in order to calculate the pressure, a probability density function (PDF) of enthalpy is needed. This was also taken from the DNS data. Average species mass fractions and temperature were calculated by,

$$\widehat{Y}_i = \int_0^1 Y_i(\xi)P(\xi)\,\mathrm{d}\xi \tag{23}$$

$$\widehat{T} = \int_0^1 T(\xi)P(\xi)\,\mathrm{d}\xi, \tag{24}$$

where $P(\xi)$ is the PDF of normalized enthalpy taken from the DNS, and $\widehat{\ }$ indicates a mean quantity for the system. An average molecular weight was then calculated using average species mass fractions calculated with Eq. (23). The average pressure was calculated from the mean quantities using $\widehat{p} = \widehat{\rho}R_\mathrm{u}\widehat{T}/\widehat{W}$, where R_u is the universal gas constant. The time rate of change in average pressure was calculated using a second order upwinding Adams–Bashforth method. With these quantities, all parameters used in the model are taken from the DNS data. For an actual application of the model in an engine simulation, models have to be provided for the enthalpy dissipation rate and the enthalpy PDF. Each of the five cases discussed below was calculated using the proposed model with the same initial conditions and chemical mechanism as the DNS.

For this model to be applied to a CFD simulation of an engine, the PDF of enthalpy and the enthalpy dissipation rate must be modeled. Although enthalpy is different from mixture fraction, both quantities could be expressed using standard models. For example, one choice for the modeled PDF of enthalpy is a beta function. The coupling of the combustion model to CFD follows the representative interactive flamelet (RIF) approach [26]. Additionally, in a real engine, both thermal and mixture composition inhomogeneities must be considered. Cook and Pitsch [27] have developed a two-dimensional flamelet-type model based on mixture fraction and a modified enthalpy. The modified enthalpy

has been formulated to remove the functional dependence of enthalpy on mixture fraction, thereby making the two-dimensions statistically independent.

4. Results

The main assumption in the derivation of the enthalpy-based flamelet model is that either diffusion is dominant in the direction normal to enthalpy iso-surfaces, or diffusion is unimportant altogether. To test the validity of this assumption in HCCI environments, the relative importance of diffusion in enthalpy-normal direction, diffusion tangential to enthalpy iso-surfaces, and the chemical source term has been assessed from the DNS data. Although the DNS data used in the present study cannot exactly represent HCCI engine conditions, it will be shown below that the data covers a broad range of conditions, ranging from the homogeneous reactor regime to the deflagration dominated regime, and might hence provide some insight. The magnitudes of the enthalpy-normal and the tangential component of the diffusion term in Eq. (1) normalized by the magnitude of the chemical source term in that equation have been evaluated locally from the DNS data for the H_2 mass fraction. From this, the PDFs of these quantities have been computed at the time of maximum heat release in the volume and the isolevel surface $Y_{H_2} = 0.00033$, which corresponds to the location of the largest magnitude of the diffusion term in Eq. (1).

The PDFs of these quantities are shown in Fig. 1. The chemical source term-normalized tangential diffusion is shown in the upper, the normalized normal diffusion in the lower panel. It is observed that for all cases the tangential diffusion component of diffusion is small compared to the chemical source term everywhere in the field. For cases 1 and 2, tangential diffusion is hardly ever larger than 5% of the chemical source term. The PDF of enthalpy-normal diffusion shows that this process is small compared to the chemical source term for case 1, but with increasing levels of inhomogeneity from case 1 to 4, this term become more significant and non-negligible. For case 4, there is a large probability for normal diffusion and the chemical source term to be of the same order of magnitude, which is characteristic of deflagrative burning. The finding that either normal diffusion is dominant or the entire diffusion process is negligible compared with the chemical source term is also supported from the joint PDF of both quantities, which is not shown here.

Another interesting observation can be made from Fig. 1. This figure shows that case 3 apparently has regions where normal diffusion is important, and other regions where transport is negligible compared with the magnitude of the

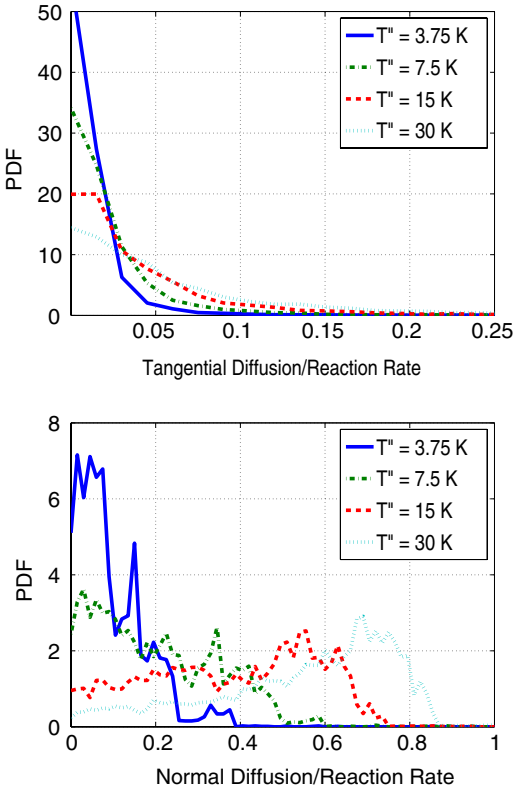

Fig. 1. DNS results for cases 1–4. (Top) PDFs of the magnitude of diffusion tangential to enthalpy iso-surfaces in the H_2 mass fraction equation normalized with the chemical source term. (Bottom) PDFs of the magnitude of diffusion in enthalpy-normal direction in the H_2 mass fraction equation normalized with the chemical source term.

chemical source term. This case is hence comprised of regions of homogeneous reactor type auto-ignition, and other regions of deflagrative burning. Previous authors have shown that for combustion in HCCI engines operated with large levels of inhomogeneities, flow and mixing are leading order effects [5,18,19]. The results shown here indicate that for such engines normal diffusion could be a significant effect while tangential diffusion is negligible.

Figure 2 shows the results of the model for cases 1–4 from left to right. The top row of plots in Fig. 2 is the heat release rate normalized by the maximum heat release rate of the homogeneous constant volume combustion case (2.27E+09 J/kg/s), and is plotted as a function of time normalized by the homogeneous ignition delay time (2.9 ms). The bottom row in Fig. 2 shows the magnitude of the diffusion term and chemical source term in the hydrogen mass fraction equation, Eq. (21). These are plotted at the time of maximum heat release for each of the four cases.

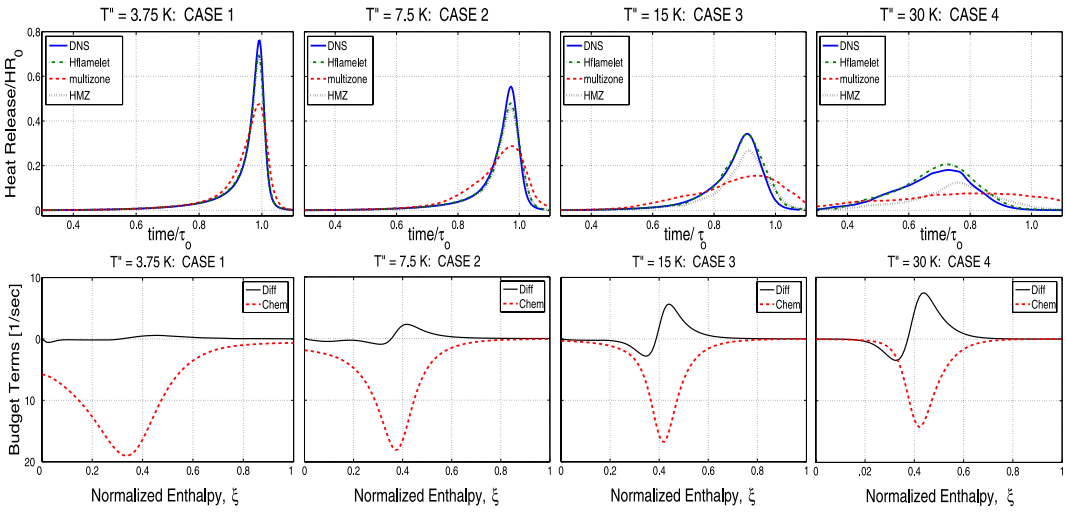

Fig. 2. (Top row) Heat release rate versus time for cases 1, 2, 3, and 4 are shown from the DNS, the enthalpy-based flamelet model (H-flamelet), the multi-zone model (multi-zone), and the enthalpy-based multi-zone model (H-MZ). (Bottom row) Budget terms for H_2 mass fraction flamelet equation from the simulation. The sum of these two terms plus the velocity term in enthalpy-space gives the rate of change.

Consistent with the DNS results for the PDFs shown in Fig. 1, as the level of enthalpy inhomogeneity increases, the relative importance of the modeled diffusion term increases. For case 1, ($T' = 3.75$ K), the diffusion term is negligible compared to the chemistry term, while the relative magnitude of the diffusion term for case 4 ($T' = 30$ K) is on the order of the chemistry term indicating propagating flame fronts. Cases 2 and 3 appear to be composed of a mixture of the two combustion modes where diffusion is non-negligible. These observations agree with the analysis of this DNS by Hawkes et al. [12], where the front propagation velocity was compared to the laminar burning velocity. A comparison of the DNS data in Fig. 1 and the model results in Fig. 2 shows that the model captures the general trend of increased importance of diffusion normal to iso-contours of enthalpy for increasing levels of thermal inhomogeneity.

The comparison of the model predictions and the DNS data of heat release rates is shown in the upper row of figures in Fig. 2. The enthalpy-based flamelet model is in excellent agreement with the DNS data for all four cases with combustion modes ranging from homogeneous auto-ignition, over mixed modes, to deflagration-type combustion. While the model was constructed to satisfy the limits associated with the homogeneous and the deflagration regimes, the results show that the model is also valid in transition regimes between these two limits.

In order to compare the enthalpy-based flamelet model to a standard type model used in HCCI simulations, results of a multi-zone model from Hawkes et al. [14] are also plotted in Fig. 2. The multi-zone calculations were initialized from the DNS data and 60,000 zones were used. The zones interacted only through pressure work since convection and diffusion between zones was not considered. Since case 1 most closely approximates the homogeneous reactor limit, which corresponds to chemical kinetics dominated combustion, the multi-zone model is capable of achieving reasonable agreement for this case. However, as the level of inhomogeneity increases and mixing becomes increasingly important from case 1 to case 4, the multi-zone results become increasingly worse while the enthalpy-based flamelet model continues to correctly model the physics. This is not too surprising, given that it was not intended to perform well in the presence of significant deflagrative burning. But the comparison demonstrates that the multi-zone model is not applicable in situations where diffusion controlled burning occurs. The results obtained from a different formulation of the multi-zone model in enthalpy space according to Eq. (11) are also shown in Fig. 2. In contrast to the MZ model, this formulation considers the temporal evolution of the enthalpy PDF. The results are improved compared with the MZ model, but the temporal development of heat release is still predicted incorrectly for the cases with higher inhomogeneities.

The bottom figure of Fig. 1 shows that for cases 2–4, there is a wide range of the relative magnitude of the diffusion term compared with the reaction rate. Similarly, Hawkes et al. [12] showed that in case 3, at a given time, the reacting fronts in different regions of the flow exhibited

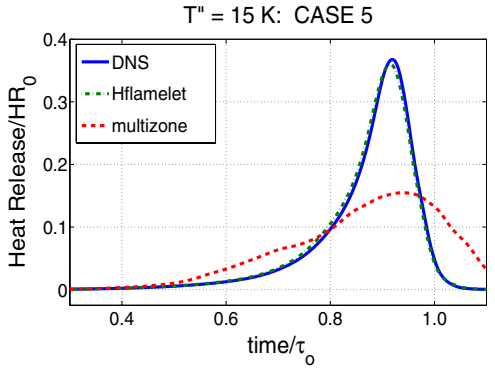

Fig. 3. Normalized heat release versus time for various times for case 5, $T' = 15\,\mathrm{K}$, unity Lewis numbers. Explanation of the legend, see Fig. 2.

varying levels of ignition-front and deflagration-type burning. For this reason, it is interesting that one flamelet with the mean enthalpy dissipation rate is capable of producing this level of agreement with the heat release rate of the DNS.

Since the enthalpy-based flamelet model in the present form does not include differential diffusion effects, a fifth DNS case (case 5) with the same conditions as case 3 ($T' = 15K$), but with unity Lewis numbers was also investigated. The enthalpy-based flamelet model and DNS heat release rates for case 5 are plotted in Fig. 3. The heat release rate plot shows almost indistinguishable results from the DNS data, while the multi-zone model predicts a much lower heat release rate. This demonstrates that the slight discrepancies seen in Fig. 2 are mainly due to the unity Lewis number assumption. However, this assumption could be more relevant for higher Reynolds number cases typical of real engines, where molecular transport effects become less important.

5. Conclusions

An enthalpy-based flamelet model for auto-ignition of mixtures with initial temperature fluctuations was presented and applied to five DNS cases with varying levels of thermal inhomogeneity. These cases covered a range of combustion modes from mostly homogeneous auto-ignition or ignition fronts to mostly deflagration-type combustion. In the mostly homogeneous auto-ignition case, $T' = 3.75\,\mathrm{K}$, the chemical source term in the enthalpy-based flamelet equation for hydrogen was dominant over the diffusion term. For the mostly deflagration case, $T' = 30\,\mathrm{K}$, these terms were of the same order. The case with $T' = 15\,\mathrm{K}$, consisted of a mixed mode of both ignition-fronts and deflagrations, where the diffusion term was smaller than the chemical source term, yet it was shown to be important. The enthalpy-based flamelet model showed good agreement with DNS heat release rates for all five cases. This model was constructed to accurately model the homogeneous reactor and the diffusive burning combustion limits. The agreement with DNS data over a range of these regimes indicates that the model is capable of capturing the physics associated with both of these limits as well as mixed regimes. The multi-zone model only showed good agreement with DNS for the chemical kinetics dominated case. For cases where mixing is important, the multi-zone model fails to represent the combustion accurately. Some discrepancy between the enthalpy-based flamelet model and the DNS data was observed for the four cases where the DNS included differential diffusion effects. However, the DNS case with unity Lewis number was in near perfect agreement with the DNS. At larger Reynolds numbers the non-unity Lewis number effects are not as significant and, therefore, this model is expected to perform well.

Acknowledgments

This work was funded in part by Robert Bosch Corporation's Research and Technology Center in Palo Alto, California. The authors would like to thank the RTC Flameless Combustion group, Dr. Aleksandar Kojić, Dr. Jasim Ahmed, and Dr. Sungbae Park for helpful discussions and comments. The work at SNL was supported by the Division of Chemical Sciences, Geosciences and Biosciences, the Office of Basic Energy Sciences, the U.S. Department of Energy. The authors acknowledge fruitful discussions with Drs. Ramanan Sankaran, John Dec, and Magnus Sjöberg.

References

[1] F. Zhao, T. Asmus, D. Assanis, J. Dec, J. Eng, P. Najt, *Homogeneous charge compression ignition (HCCI) engines, key research and development issues*, Society of Automotive Engineers, Inc., Warrendale, PA, 2002, pp. 1–14 and 531–541.
[2] A. Hultqvist, M. Christenson, B. Johansson, M. Richter, J. Nygren, J. Hult, M. Alden, SAE Technical Paper 2002-01-0424, 2002.
[3] J. Dec, SAE Technical Paper 2002-01-1309, 2002.
[4] K. Epping, S. Aceves, R. Bechtold, J. Dec, SAE Technical Paper 2002-01-1923, 2002.
[5] M. Christensen, B. Johansson, SAE Technical Paper 2002-01-2864, 2002.
[6] S. Aceves, D. Flowers, C. Westbrook, J. Smith, W. Pritz, R. Dibble, M. Christensen, B. Johansson, SAE Technical Paper 2000-01-0327, 2000.
[7] S. Aceves, D. Flowers, J. Martinez-Frias, J. Smith, C. Westbrook, W. Pritz, R. Dibble, J. Wright, W.

Akinyemi, R. Hessel, SAE Technical Paper 2001-01-1027, 2001.
[8] S. Aceves, D. Flowers, J. Martinez-Frias, R. Dibble, M. Christensen, B. Johansson, R. Hessel, SAE Technical Paper 2002-01-2869, 2002.
[9] S. Kong, R. Reitz, *Proc. Combust. Inst.* 29 (2002) 663–669.
[10] D. Cook, P. Pepiot, H. Pitsch, The Proceedings of The Joint Meeting U.S. Sections Combustion Institute, 2005.
[11] D. Cook, H. Pitsch, SAE Technical Paper 2005-01-3537, 2005.
[12] J.H. Chen, E.R. Hawkes, R. Sankaran, S.D. Mason, H.G. Im, *Combust. Flame* 145 (1–2) (2006) 128–144.
[13] E.R. Hawkes, R. Sankaran, P.P. Pebay, J.H. Chen, *Combust. Flame* 145 (1–2) (2006) 145–159.
[14] E. Hawkes, R. Sankaran, J. Chen, H. Im, The Proceedings of The 4th Joint Meeting of U.S. Sections of The Combustion Institute, 2005.
[15] P. Najt, D. Foster, SAE Technical Paper 830264, 1983.
[16] M. Noguchi, Y. Tanaka, T. Tanaka, Y. Takeuchi, SAE Technical Paper 790840, 1979.
[17] N. Iida, SAE Technical Paper 972071, 1997.
[18] S. Hong, D. Assanis, M. Wooldridge, SAE Technical Paper 2002-01-1112, 2002.
[19] S. Kong, C. Marriot, C. Rutland, R. Reitz, SAE Technical Paper 2002-01-1925, 2002.
[20] R. Osborne, G. Li, S. Sapsford, J. Stokes, T. Lake, M. Heikal, SAE Technical Paper 2003-01-0750, 2003.
[21] Y. Zel'dovich, *Combust. Flame* 39 (2) (1980) 211–214.
[22] A. Liñan, F. Williams, *Combust. Sci. Tech.* 105 (4–6) (1995) 245–263.
[23] N. Peters, *Combust. Sci. Tech.* 30 (1–6) (1983) 1–17.
[24] N. Peters, *Prog. Energy Sci.* 10 (1984) 319–339.
[25] M. Mueller, T. Kim, R. Yetter, F. Dryer, *Intl. J. Chem. Kinetics* 31 (2) (1999) 113–125.
[26] H. Pitsch, H. Barths, N. Peters, SAE Technical Paper 962057, 1996.
[27] D.J. Cook, H. Pitsch, *Western States Section of the Combustion Institute*, Boise, Idaho 06S-08, 2006.

Comments

Simone Hochgreb, Cambridge University, UK. What is the potential efficiency of this method relative to methods that handle chemistry/reaction rate terms directly such as CMC?

Reply. For the model presented here, two additional scalar equations without chemical source terms have to be solved. Hence, the computational overhead is very modest. A conditional moment closure (CMC) model that handles the types of flows we have discussed does not exist. CMC models are typically formulated to describe variations in mixture fraction, which is constant in our case. However, one could formulate a model that uses the enthalpy as a conditioning variable, which would lead to equations similar to the model we have presented, in case similar closure assumptions are used. However, the CMC equations are four-dimensional and time dependent. Also, one of these equations has to be solved for each species in the mechanism. The computational requirements for this would be enormous. These equations could then be solved on a mesh that is courser than the fluid flow mesh, which reduces the computational time. But this could be quite complicated given the complex geometry and moving boundaries of piston and valves.

•

Derek Bradley, Leeds University, UK. With lean hydrogen–air mixtures an auto-ignition front and a flame front can co-exist. However, with very lean hydrocarbon–air mixtures it is more probable that the turbulence would cause any embryonic flame to be extinguished.

Reply. We have found that depending on the conditions small-scale flame fronts can be dominant or small-scale ignition fronts, or both can exist at the same time. The main point of our paper is not that one of these is more important, but that the model can give excellent predictions in both limiting regimes and in the mixed regime, and can therefore be used irrespective of which mode is more important. However, we have performed simulations for a typical HCCI geometry with a very lean propane mixture, and found that even under these conditions, the small-scale flame propagation mode was dominant.